SolarPACES 2024, 30th International Conference on Concentrating Solar Power, Thermal, and Chemical Energy Systems

AI in Concentrating Solar Technology

https://doi.org/10.52825/solarpaces.v3i.2406

Published: 25 Nov. 2025

AI-Based Generative Geometrical Design of Concentrated Solar Thermal Tower Receivers

Jorge Moreno García-Moreno[1], Kypros Milidonis[1,*], Mihalis Nikolaou[1], and Wojciech Lipinski[1]

[1]The Cyprus Institute, CY

*Correspondence: Kypros Milidonis, k.milidonis@cyi.ac.cy

Abstract. An artificial intelligence (AI) aided generative design workflow for the optimization of cavity receivers for concentrated solar thermal (CST) energy systems is presented. The workflow integrates the Non-dominated Sorting Genetic Algorithm III (NSGA-III) with generative design methodologies and optical evaluation through Monte-Carlo ray-tracing in an interoperable way, to optically optimize the geometry of cavity receivers according to a set of objective functions for a given heliostat field. As a demonstrator test case, the workflow is used to provide an optimal geometrical design of a cavity receiver given the Cyprus Institute's PROTEAS heliostat field. It is shown that the workflow is able to generate unconventional, non-intuitive and efficient receiver designs in an automated manner, which are often not conceived by traditional design approaches.

Keywords: Concentrated Solar Power, Concentrated Solar Thermal, Thermal Receivers, Generative Design, Artificial Intelligence, NSGA-III.

1. Introduction

The rapid advancements in the field of Artificial Intelligence (AI) are significantly contributing to the progress in science and technology. Utilization of AI techniques in the renewable energy sector has given rise to a wide number of applications, with approaches ranging from weather forecasting and predictive control, to transforming design and optimization of components and systems [1]. Furthermore, the increased accessibility of high-performance computing (HPC) provides the necessary computational resources for AI to reach its full potential, which in turn enables the development and deployment of large-scale, data-intensive AI applications, facilitating research and innovation in AI-related fields. AI has been identified and proven as a valuable tool for addressing challenges within the concentrating solar thermal (CST) sector [2], including the design and optimization of heliostat fields and related thermal components [3], maintenance and diagnostics [4], and system design and optimization [5]. In the context of engineering design, the integration of computer-based intelligence and generative design lies in the ability to use AI algorithms to automate the creation, optimization, and evaluation of design solutions through intelligent decision-making, allowing for more efficient and innovative design processes. This paper presents a novel AI-based methodology for the generative design of CST tower receivers for the geometrical design of cavity receiver. Each step of the fully automated methodology is presented, and the application of the methodology for the optimization of a cavity receiver is demonstrated for a given north-type heliostat field.

2. The AI-based generative design methodology

A simplified representation of the AI-based receiver generative design methodology developed is shown in Figure 1. The design process starts with the definition of the CST tower configuration and includes the definition of all parameters that constitute the plant. They include: (1) the heliostat field along its properties (mirror reflectivity, tracking type, etc); (2) an initial receiver geometry parametrization; (3) the atmospheric conditions; (4) the geographic location of the plant; and (5) the sun's position and the corresponding direct normal irradiation (DNI) at a given time or at a set of sun positions that define a typical meteorological year. In sequence, a Monte-Carlo ray-tracing scene that fully replicates the configuration of the plant is automatically constructed, in which the optical performance of the receiver is numerically evaluated. The Free/Libre and Open Source Software (FLOSS) Tonatiuh++ ray tracer [6] is used in this step. Next, the AI-based, non-dominated sorting genetic algorithm III (NSGA-III) takes over for multi-objective multi-variable evaluation of the candidate receiver geometries according to the set objective functions. One remarkable feature of NSGA-III is the implementation of the crowding distance method, which promotes the exploration of the pareto front by avoiding locality. Consequently, a new receiver design population is automatically generated and fed back into the initial step for re-evaluation. The result is a multidimensional (according to the number of set objective functions) pareto front with candidate receiver geometries. The candidate receiver geometries are generated through multiple axial control cross-sections (defined by one or more parameters) along the receiver's length, which are subsequently interpolated to generate the surface mesh of the receiver geometry. During this interpolation step, spatial resolution can be defined to determine the geometry's resolution. The individual steps of the workflow are presented in sections that follow.

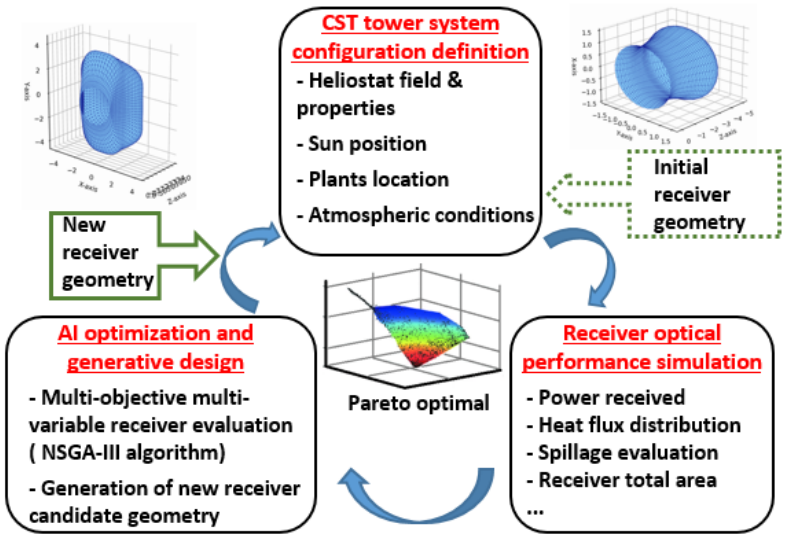

Figure 1. *Overview of the AI-based generative design workflow*

3. The demonstration test case

For demonstrating the methodology, the Cyprus Institute's (CYI) PROTEAS heliostat field [7] has been employed. The PROTEAS' heliostat field is composed of 50 CSIRO single rectangular facet heliostats, each of 5 m^2 in mirror area, totaling thus a mirror area of 250 m^2. The heliostats are arranged along 5 rows on a slightly hilly terrain as shown in *Figure 2.* The PROTEAS heliostat field and tower, a) actual configuration, b) the Tonatiuh++ raytracing scene developed as an exact replica.The field is equipped with an 18 m tall tower, hosting a cavity receiver whose inlet aperture center is located at 14 m. A single aiming point aiming strategy is adopted, with the aiming point being the center of the inlet aperture of the receiver.

For the purposes of the workflow, an exact ray-tracing PROTEAS scene has been developed in Tonatiuh++ Monte-Carlo ray tracer, as shown in *Figure 2*b. In the details of the ray-tracing scene, the Buie sunshape was selected with a circumsolar ratio (CSR) of 2%, while the reflectivity of the heliostat's mirrors was set to 95% with mirror slope error deviation of 2 mrad. During the optimization process, a single point aiming point and sun position (180° azimuth and 70° elevation) has been employed with a nominal value of Direct Normal Irradiation (DNI) equal to 1000 W/m^2. A clear day polynomial distribution model was adopted for the atmospheric attenuation [8]. Finally, the reflectivity of the internal surfaces of the receiver was set to 60%.

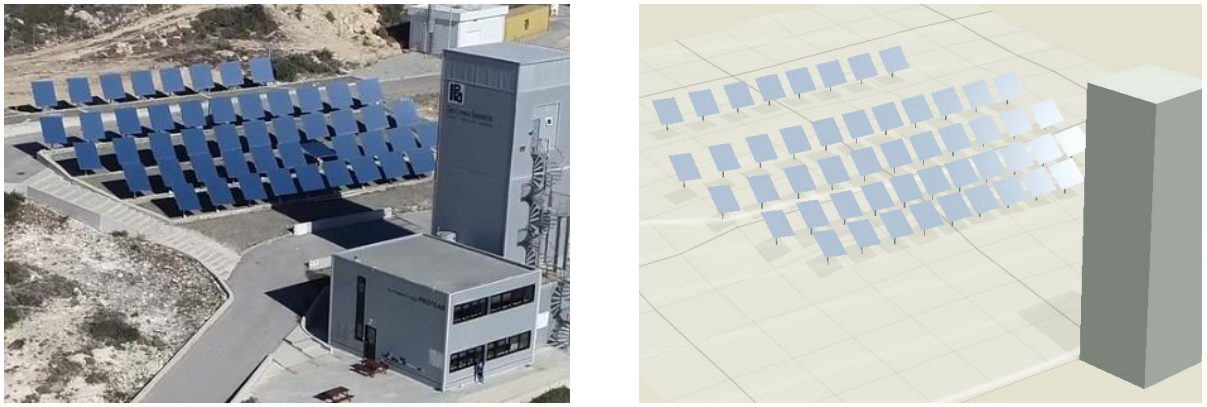

(a) (b)

Figure 2. *The PROTEAS heliostat field and tower, a) actual configuration, b) the Tonatiuh++ raytracing scene developed as an exact replica.*

4. Parametrization of the receiver geometry

As described in section 2, the candidate receiver geometries are generated through multiple axial control cross-sections (defined by one or more parameters) along the receiver's length, which are subsequently interpolated to generate the surface mesh of each candidate receiver geometry. Two different parametrization methods being valid for cavity receivers have been investigated in this study, the axisymmetric type receivers and the biplane symmetry type receivers. Both parametrization methods are based on multiple axial control cross-sections along the length of the receiver, which are later interpolated to generate the receiver design.

4.1 Axisymmetric receivers

The control cross-sections of the axisymmetric receiver parametrization method are circumferences defined by two variables per each cross-section, i.e. the cross-section axial Z-axis coordinate along the receiver's length, and the circumference radius as shown in *Figure 3a*. Given a set of multiple axial control cross-sections and their corresponding location along the receive length, the Akima interpolation [9] scheme is performed between the different sections to generate the profile of the receiver. The result is a generatrix interpolation that when rotated around the central axis running along the length of the receiver, generates a revolved axisymmetric receiver geometry as shown in *Figure 3c.*

4.2 Bi-planar symmetry receivers

In this receiver parametrization method, the control cross-sections are rounded corner rectangles, defined by four variables: the axial Z-axis coordinate along the receiver's length, the width

(x-axis) and height (y-axis) coordinates, and the corners radius. Similarly to axisymmetric receivers, the Akima interpolation scheme is performed between the different sections to generate the shape of the receiver. An example control cross-section and receiver shape are shown in *Figure 4.*

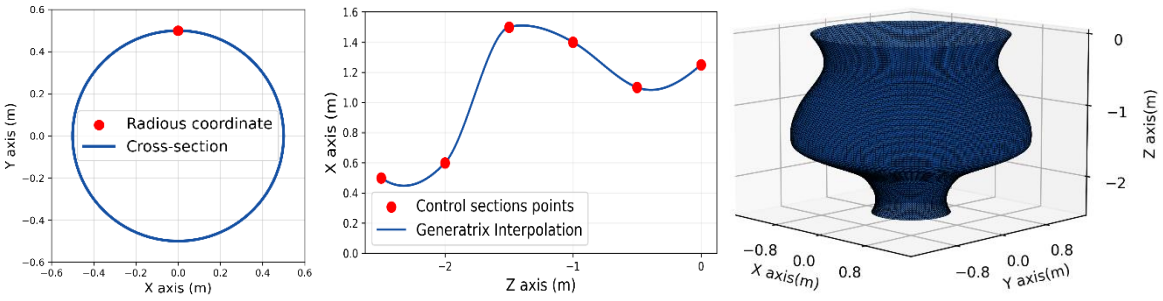

(a) *(b)* *(c)*

Figure 3. *Receiver axisymmetric parametrization method, a) control cross-section b) Cross-section Akima Interpolation, c) revolved receiver geometry obtained as an object of rotation.*

For both parametrization methods, the resolution of the obtained receiver geometries was controlled during the Akima interpolation step. At a following step, the resulted receiver geometries are then exported as wavefront object file format (i.e. obj) meshes, which were then automatically imported in the PROTEAS Tonatiuh++ scene to perform the necessary optical simulations. Each candidate receiver geometry was automatically spatially positioned at the location of the receiver, matching the center of the receiver inlet aperture to the heliostat field aiming point.

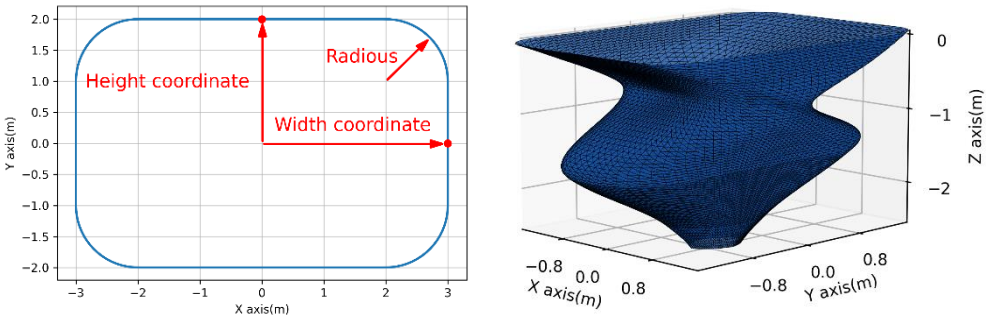

(a) *(b)*

Figure 4. *Bi-plane symmetry parametrization, a) Control cross-section. b) Receiver geometry*

5. The Non-dominated Sorting Algorithm III (NSGA-III)

Derived from the evolution theory defined by Darwin, genetic algorithms (GAs) are metaheuristic search and optimization algorithms in which a population (i.e. a set of receiver candidates) is firstly generated; the individuals (i.e. receivers) composing the population are evaluated; the best performers individuals are considered as the parents that will combine its characteristics (genes) to create the individuals of the next generation in the reproduction process. Each individual in the population is considered a solution, i.e. a receiver design, and its parametrization are the genes that may be passed to the next generation individuals. The ”non-dominated sorting genetic algorithm (NSGA)” [10] constitutes a variant of GAs, that are able to better address multi-objective optimization problems. NSGA incorporates the concept of non-dominated sorting to rank the best solutions in a population. In this formulation, a solution is considered to dominate if it outperforms, and the best solutions are then the non-dominated ones. Considering that an individual is not-dominated if no other, in the population, has a better evaluation in at least one objective function while the other objective function evaluation is equal

or worse. In that case, the first front is composed of all the individuals that are not dominated in the population; the second front are the non-dominated solutions in the population when the first front individuals are extracted from the population; and so, until all the individuals are sorted in multiple fronts. The optimization problem presented in this article is bounded by three objectives functions as it is discussed later on, thus the NSGA-III formulation [11] was deemed to be the best approach to be integrated in the optimization workflow.

5.1 Objective functions

The optimization workflow seeks to find the optimal cavity receiver geometry for the given heliostat field based on three objective functions: maximization of the power absorbed by the receiver, maximization of the uniformity of the heat flux distribution at the internal surfaces of the receiver, and minimization of the receiver's area, which is directly related to receiver cost. The power absorbed by the receiver is the sum of all rays absorbed at the receiver's internal surface multiplied by the power carried by each ray:

$$\max P_{absorbed} = P_{ray} * \sum rays_{absorbed} \quad (1)$$

A non-uniform heat flux distribution, can lead to sudden temperature gradients resulting to structural failure of the receiver. Thus, a metric expressing the standard deviation of the heat flux (HF_{std}) at all faces (F) conforming the receiver surface mesh, being (hf_i) the heat flux in each face (i) and ($\overline{hf}$) the average heat flux in the receiver was derived as follows:

$$\min HF_{std} = \sqrt{\frac{\sum_{i=1}^{F}\left(hf_i - \overline{hf}\right)^2}{F}} \quad (2)$$

An immensely large receiver will capture the maximum available power while achieving a good uniformity value in the HF_{std} metric, however this will lead to increased receiver cost. For that reason, the third objective function seeks for the minimization of the receiver absorbing area as follows:

$$\min A_{receiver} = \sum_{i=1}^{F} A_i \quad (3)$$

5.2 Search Space - Variables bounds

The receiver parametrization methods as described in section 3, allow for a large design space to be explored to find optimal receiver designs. This implies large combinatorics, demanding thus enormous computational efforts for evaluating all the generated designs, given the fact that all receiver candidates are optically simulated and evaluated through computationally expensive Monte-Carlo ray-tracing. Combinatorics reduction is a key factor to minimize the computational cost and time required for the NSGA-III to converge. For that reason, the search space must be adequately dimensioned.

The maximum axial coordinate, i.e. the receiver length, is bounded to a maximum of 3 m, and, while each control cross-section (s) can be along the z-axis in any position, its position

must be always in an increasing order. The maximum circumference radius (CR_s) (in the axisymmetric receiver parametrization), height (H_s) and width (W_s) coordinate; and radius (R_s) (in the bi-plane symmetry parametrization) can have a maximum value of 2 m. In addition, the decimal precision is stablished to ± 1 cm to avoid the evaluation of almost identical receiver designs that in practice will have the same performance. The entire search space is summarized in *equations (4)-(9)*.

$$Z_{s-1} < Z_s < Z_{s+1} \quad (4)$$

$$0.00 \leq Z_{max} \leq 3.00 \quad (5)$$

$$0.00 \leq CR_s \leq 2.00 \quad for\ s = 1, \dots, S \quad (6)$$

$$0.00 \leq R_s \leq 2.00 \quad for\ s = 1, \dots, S \quad (7)$$

$$0.00 \leq H_s \leq 2.00 \quad for\ s = 1, \dots, S \quad (8)$$

$$0.00 \leq W_s \leq 2.00 \quad for\ s = 1, \dots, S \quad (9)$$

5.3 Hyperparameters

During the initialization of the NSGA-III, inherent hyperparameter values were defined, including reference directions, population and offspring sizes, crossover and mutation probabilities, etc. The lack of information regarding the performance of metaheuristic algorithms in the exact problem being tackled in this study led to the use of standard approaches as commonly employed in the literature. The reference directions structure used are the known as "Das and Dennis" [12] for a three-dimensional space and 5 partitions. A population size of 500 individuals is employed, with this size being larger than the usual population size employed in literature (i.e. close to 200), to avoid the discard of possible different design topologies competing against each other along the generations. The offspring size was set to 500 to avoid elitism during the first generations, allowing a faster convergence of the algorithm. The probabilities employed during the cross-over and mutation operators are set to 0.6.

6. Results and discussion

Figures 5a and 5c depict the evolution of the NSGA-III algorithm along the generations by means of pareto optimal fronts, for the axisymmetric and bi-planar symmetry receivers respectively. The 3D pareto front is plotted against the three set objective functions, i.e. the flux uniformity, the power absorbed and the surface area of the receiver. It can be seen that by starting from random receiver geometries, the algorithm is converging to optimal receiver designs in approximately 60 generations. Respectively, *Figures 5b and 5d* only show the evaluated receiver designs ranked per front, since the algorithm is discarding bad performing receiver candidate geometries in every generation.

As examples of optimal receiver designs, *Figure 6* depicts two selected receiver geometries as generated for the axisymmetric and bi-planar symmetry receivers respectively. The axis-symmetric receiver shown in *Figure 6a* has an absorbing surface area of 22.64 m^2, allowing a power absorption of 200.7 kW with a corresponding heat flux distribution HF_{std} of 9.9 kW/m^2 and an optical efficiency of 92.5%. On the other hand, the bi-plane symmetry receiver has an absorbing surface area of 22.68 m^2, absorbs a power of 207.3 kW with an HF_{std} of 9.5 kW/m^2, while achieving an optical efficiency of 93.4%.

The bi-plane symmetry parametrization receiver performs slightly better than the axis-symmetric receiver, allowing a 3.2% more power absorbed in with a slightly more uniform heat flux distribution, corresponding to a 4% decrease in HF_{std}. It is evident that due to the increased flexibility of the bi-planar receiver parametrization method, the algorithm can explore a wider variety of receiver geometry candidate solutions, when compared to the axisymmetric receiver parametrization in which the receiver geometry is just an object of rotation.

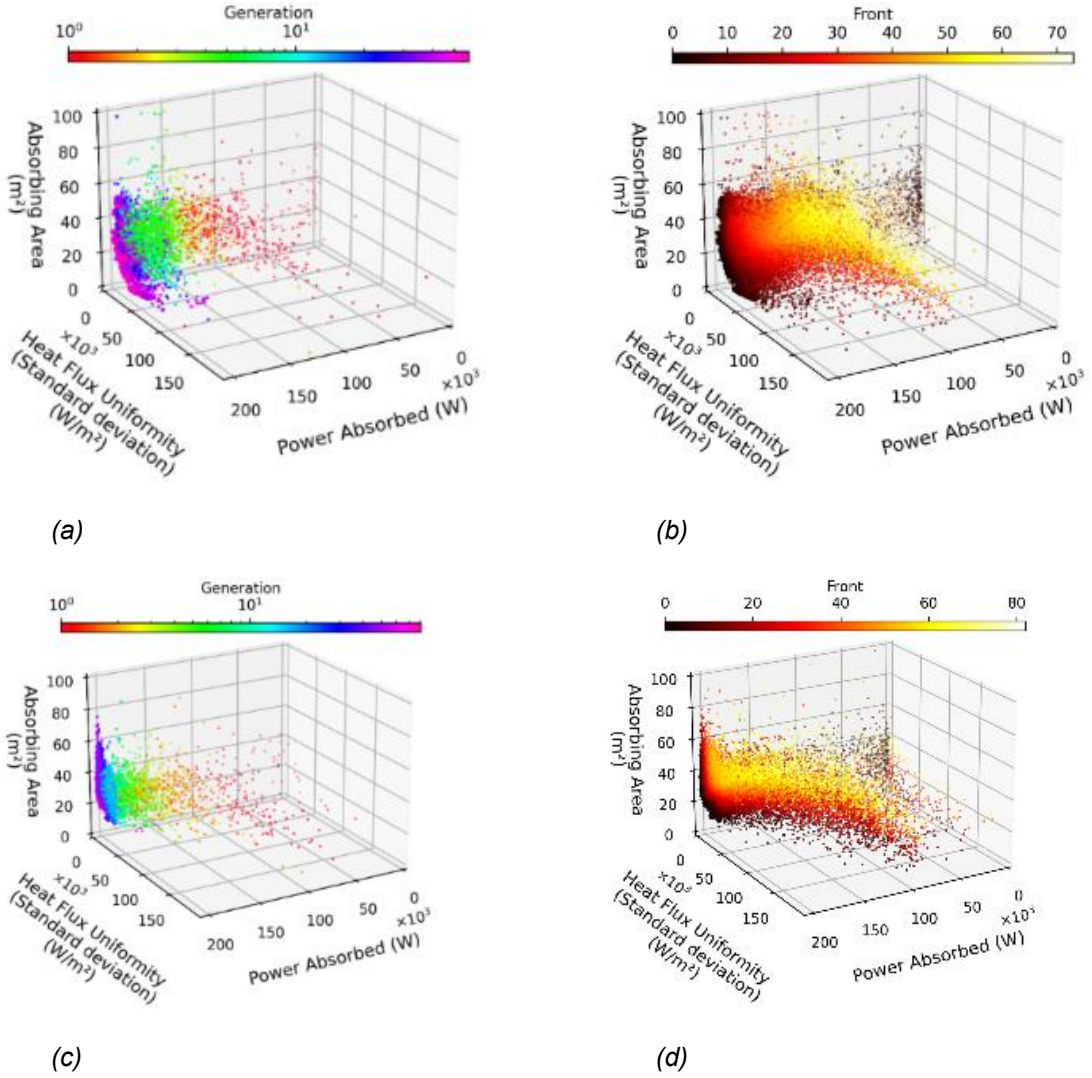

Figure 5. *NSGA-III evolution and all evaluated receivers, a) Axisymmetric NSGA-III evolution. b) Axisymmetric fronts. c) Bi-plane symmetry NSGA-III evolution. d) Bi-plane symmetry fronts*

Although the material reflectivity is set to 60%, the optical efficiencies of the generated receiver geometries are higher than 92%. This means, that according to the set objective functions, the algorithm seeks to create a ''light trap'', generating designs that ensure multiple reflections inside the receiver cavity in order to maximize the flux uniformity on the receiver surfaces, while, at the same time minimizing the size of the inlet aperture of the cavity to limit as much as possible the number of rays that are reflected back into the environment, i.e. to maximize the power absorption. Of course, the fact that a single point aiming strategy is employed with no heliostat tracking errors, along with the fact that optical simulations are performed for a single sun position, also contribute towards the generation of such optimal receiver geometries. As a reference of the performance of the two receiver optimal designs, *Figure 7* depicts examples of the Tonatiuh++ ray-tracing scene in which the two optimal receiver geometries are positioned at the receiver spatial location.

7. Conclusions

A workflow integrating synergies between artificial intelligence and generative design approaches have been employed in the present study for the geometrical optimization of cavity receivers. Starting from a set of completely random geometries, the methodology has proven to be able to converge to receiver geometries that are meaningful with respect to the set objective functions and the respective search space bounds. Although the methodology employed here is applied to the geometrical design optimization of cavity receivers for CST systems, the workflow can be similarly applied to other Concentrating Solar Thermal (CST) components, such as the optimization of external receivers, secondary reflectors of Linear Fresnel systems, solar reactors/furnaces, etc.

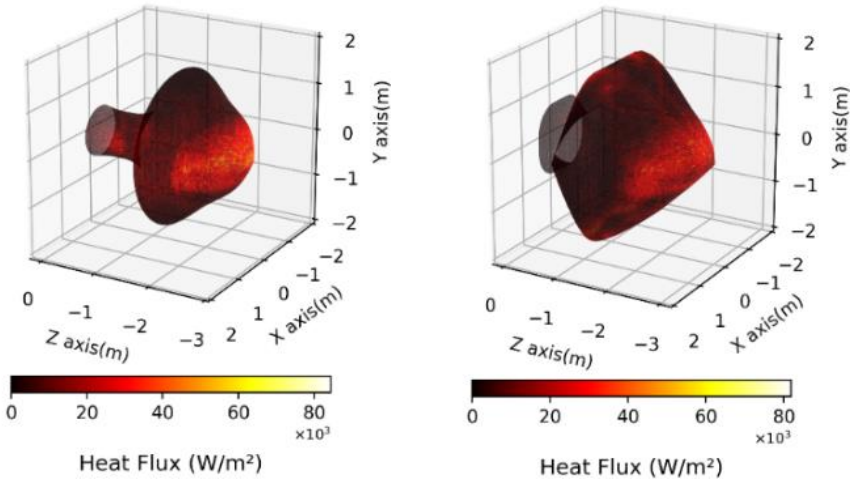

Figure 6. *Heat flux distribution. a) Axisymmetric receiver. b) Bi-plane symmetry*

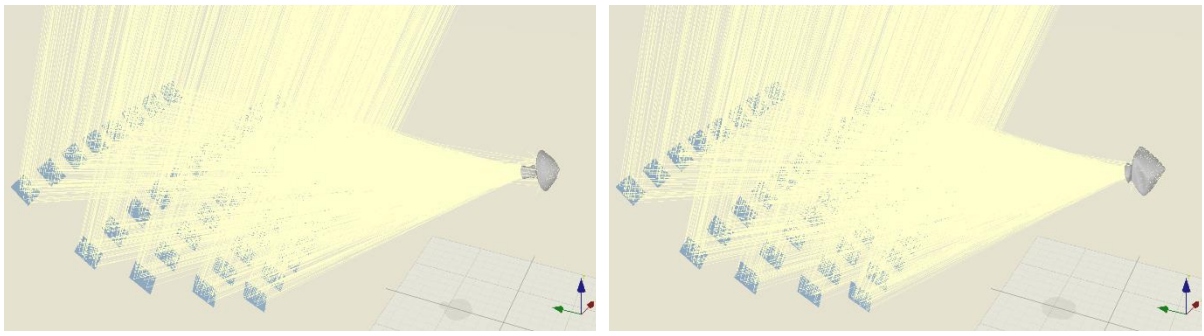

Figure 7. *Tonatiuh++ raytracing scene, a) Axisymmetric receiver. b) Bi-plane symmetry*

Author contributions

Jorge Moreno García-Moreno: Conceptualization, data curation, formal analysis, methodology, software, writing-original draft / **Kypros Milidonis:** Conceptualization, methodology, funding acquisition, project administration, supervision, writing-original draft, writing-review & editing / **Wojciech Lipinski:** project administration, supervision, writing-review & editing, **Mihalis Nikolaou:** supervision, writing-review & editing.

Competing interests

The authors declare that they have no competing interests.

Funding

This study was funded from the European Horizon 2020 research and innovation programme under the Marie Skłodowska-Curie grant agreement No 101072537.

References

[1] S. Kr, J. Bilalovic, A. Jha, N. Patel and H. Zhang, “Renewable energy: Present research and future scope of Artificial Intelligence,” Renewable and Sustainable Energy Reviews, vol. 77, pp. 297-317, 2017.
[2] K. Milidonis, M. J. Blanco, V. Grigoriev, C. F. Panagiotou, A. M. Bonanos, M. Constantinou, J. Pye and C.-A. Asselineau, “Review of application of AI techniques to Solar Tower Systems,” Solar Energy, vol. 224, pp. 500-515, 2021.
[3] M. A. Al-Sulaiman and A. Fahad, “Optimization of heliostat field layout in solar central receiver systems on annual basis using differential evolution algorithm,” Energy Conversion and Management, vol. 95, pp. 1-9, 2015.
[4] T. Ashley, E. Carrizosa and E. Fernández-Cara, “Heliostat field cleaning scheduling for Solar Power Tower plants: A heuristic approach,” Applied Energy, vol. 235, pp. 653-660, 2019.
[5] Y. Luo, T. Lu and X. Du, “Novel optimization design strategy for solar power tower plants,” Energy Conversion and Management, vol. 177, pp. 682-692, 2018.
[6] V. Grigoriev, M. Blanco and K. Milidonis, “Tonatiuh++ Solar Raytracer (v0.1.8.17),” Zenodo, 2022.
[7] A. M. Bonanos and C. N. Papanicolas, “The PROTEAS facility heliostat field: Layout and performance prediction,” in 5th International Conference on Renewable Energy Sources & En-ergy Efficiency, Nicosia, Cyprus, 2016.
[8] J. Ballestrín and A. Marzo, “Solar radiation attenuation in solar tower plants,” Solar Energy, vol. 86, pp. 388-392, 2012.
[9] H. Akima, “A New Method of Interpolation and Smooth Curve Fitting Based on Local Procedures,” J. ACM, vol. 17, pp. 589-602, 1970.
[10] N. Siinivas and K. Deb, “Muiltiobjective Optimization Using Nondominated Sorting in Genetic Algorithms,” 1994.
[11] K. Deb and H. Jain, “An evolutionary many-objective optimization algorithm using reference-point-based nondominated sorting approach, Part I: Solving problems with box constraints,” IEEE Transactions on Evolutionary Computation, vol. 18, pp. 577-601, 2014.
[12] I. Das and J. E. Dennis, “Normal-Boundary Intersection: A New Method for Generating the Pareto Surface in Nonlinear Multicriteria Optimization Problems,” SIAM Journal on Optimization, vol. 8, pp. 631-657, 1998.